Effects of doping, Stone–Wales and vacancy defects on thermal conductivity of single-wall carbon nanotubes*

Feng Dai-Li(冯黛丽), Feng Yan-Hui(冯妍卉)†, Chen Yang(陈 阳), Li Wei(李 威), and Zhang Xin-Xin(张欣欣)

School of Mechanical Engineering, University of Science and Technology Beijing, Beijing 100083, *China*

(Received 30 May 2012; revised manuscript received 15 June 2012)

The thermal conductivity of carbon nanotubes with certain defects (doping, Stone–Wales, and vacancy) is investigated by using the non-equilibrium molecular dynamics method. The defective carbon nanotubes (CNTs) are compared with perfect tubes. The influences of type and concentration of the defect, length, diameter, and chirality of the tube, and the ambient temperature are taken into consideration. It is demonstrated that defects result in a dramatic reduction of thermal conductivity. Doping and Stone–Wales (SW) defects have greater effect on armchair tubes, while vacancy affects the zigzag ones more. Thermal conductivity of the nanotubes increases, reaches a peak, and then decreases with increasing temperature. The temperature at which the thermal conductivity peak occurs is dependent on the defect type. Different from SW or vacancy tubes, doped tubes are similar to the perfect ones with a sharp peak at the same temperature. Thermal conductivity goes up when the tube length grows or diameter declines. It seems that the length of thermal conductivity convergence for SW tubes is much shorter than perfect or vacancy ones. The SW or vacancy tubes are less sensitive to the diameter change, compared with perfect ones.

Keywords: thermal conductivity, carbon nanotubes, Stone–Wales defects, molecular dynamics

PACS: 65.80.–g, 61.48.De, 63.22.Gh, 02.60.Cb **DOI:** 10.1088/1674-1056/22/1/016501

1. Introduction

Carbon nanotubes (CNTs) have attracted more and more attention for their excellent performance in mechanical behavior, and thermal and electrical properties since they were discovered in 1991.[1] In particular, it is widely accepted that carbon nanotube is one of the best thermal conductors that can be used as the filling substance of composite materials or nanofluids[2,3] to enhance their thermal performance. Described as one-dimensional, hexagon-connected, seamless cylindrical structure, CNTs are not absolutely perfect due to the presence of certain defects. It has been exposed in experiments that preparing nanotubes or scanning nanotubes with an atomic force microscope (ATM) or a scanning tunneling microscope (STM) can cause structural defects, and even damage[4,5] in nanotubes.

Intensive studies have been undertaken investigate the defects and they can be mainly classified into four groups: topological defects, doping with other elements, rehybridization defects, and incomplete bonding defects. In addition, intra-molecular junctions and inter-molecular junctions are two other special defects which include one or more of the basic defects mentioned above. These defects have a strong effect on a CNT's physical and chemical properties. Furthermore, the existence of defects could easily increase some particular performances, which allow more potential applications of CNTs.

Some studies show the dependence of thermal conductivity of nanotubes on structural defects. There is sharp discontinuity in the temperature profile at hetero-junction defects, leading to lower value for the thermal conductivity of nanotubes with defects.[6,7] A prediction from Bi *et al.*[8] has stated that 1% ^{13}C doping would result in a 30% decrease of thermal conductivity, while vacancy CNTs with 0.25% defect concentration would bring about a 60% decrease. Moreover, Che *et al.*[9] have analyzed the impact on thermal conductivity of CNTs with vacancy defects and with Stone–Wales (SW) defects. He found that both defects would lead to a poor performance in heat transfer, and vacancies can have a more noticeable influence. Kondo *et al.*[10] noticed that the thermal conductivity falls by 25% under the condition of a 1% vacancy defect concentration. Research by Zhang and Li[11] has pointed out that thermal conductivity of CNTs can decline by as much as 40% under 40%–50% ^{14}C doping. Recently, Li *et al.*[12] simulated the influences of point defects (vacancy, doping, and adsorption) on the thermal conductivity of carbon nanotubes by using an orthogonal array testing strategy. The results showed that defect type has the greatest influence on the reduction of thermal conductivity, followed by the radius and the length of carbon nanotubes. To date, most of new studies on doping defects are focused on field emission properties,[13] structural stability,[14] optical properties,[15] and electrical behavior,[15,16] while discussions about thermal properties are rare.

There have been controversial conclusions among previ-

*Project supported by the National Natural Science Foundation of China (Grant Nos. 50876010 and 51176011) and the Program for New Century Excellent Talents in University of Ministry of Education of China (Grant No. NCET-08-0721).

†Corresponding author. E-mail: yhfeng@me.ustb.edu.cn

© 2013 Chinese Physical Society and IOP Publishing Ltd

ous studies on the thermal conductivity of defective nanotubes. Moreover, results and discussions have mostly concerned descriptions of the phenomena; revelations on thermal transport mechanisms are far from the expectation. Up to now, comparisons of doping, SW and vacancy CNTs have rarely been made, let alone analyzed overall under all factors (concentration, length, diameter, chirality, and ambient temperature). Thus, it is a subject that requires in-depth investigation, in order to better understand the effects of various defects, make a rational control, and use these defects. In this paper, we focus on carbon nanotubes with different defects, realize the reconfiguration of defective CNTs, simulate the thermal conductivity by using the non-equilibrium molecular dynamics (NEMD) method, and finally find the thermal response regulation of CNTs exposed to defect structures. Discussion and possible explanations are given to analyze the defect effects, which are further expected to be useful for exploring some new functional performances of CNTs and to possibly support the development of nanoscale devices.

2. Model

In this paper, three types of defects are investigated: doping defect, SW defect, and vacancy defects.

Doping defect Doping means that one or several foreign atom(s) replace the carbon atoms within the lattice structure of a CNT, as shown in Fig. 1. Doping defects commonly exist in both single-wall carbon nanotubes and multi-wall carbon nanotubes. Boron (B), nitrogen (N), and potassium (K) doping are considered in this study.

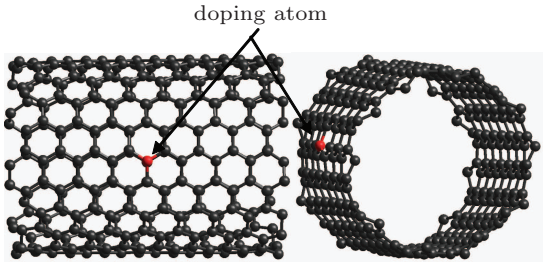


Fig. 1. (color online) Doping defects.

SW defect The Stone–Wales (SW) defect, which corresponds to a rotation of two carbon atoms with respect to the midpoint of the bond, as shown in Fig. 2, also called the 7557 defect, is a kind of crystallographic, topological defect that usually occurs in carbon nanotubes.

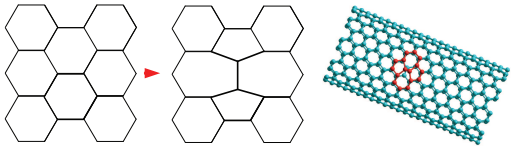


Fig. 2. (color online) Stone–Wales defects.

Vacancy defect According to previous experimental studies, carbon atoms would be released from CNTs when irradiated by electrons or ions. Therefore, vacancies are formed. Two of the surrounding three dangling bonds can link with each other to form a pentagon shape, as shown in Fig. 3.

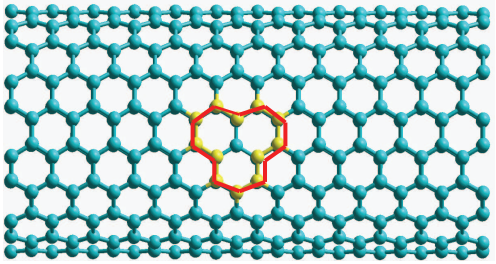


Fig. 3. (color online) Vacancy defects.

The SW and vacancy defects are very pervasive in CNTs. They can directly bring local destruction to the stable molecular structures of CNTs, which causes the energy value of system stability to decline sharply. Meanwhile, both SW and vacancy defects will damage the perfect hexagonal structure, weaken the interactions of carbon–carbon (C–C) bonds among adjacent atoms, and give a higher degree of freedom to those atoms in defect positions.

The model of a single-wall CNT (10, 10) (see Fig. 4) has a radius of 4.13 Å, with C–C bond length of 1.42 Å. A ring area of van der Waals thickness of 3.4 Å is employed as the cross-sectional area of the nanotube. There exist one or more defect(s) in the middle of the nanotube. The nanotube is divided into three parts: adiabatic wall at each end of the tube, thermostat area adjacent to the adiabatic wall, and the free part in the center. An adiabatic wall is used to make the atoms in thermostat areas steady, and equalize the forces applied on them. In our simulations, we assign different temperatures, T_{L} and T_{H} ($> T_{\mathrm{L}}$), to the left- and right-end layers of CNTs to generate a thermal current through the CNTs. The temperatures of the thermostat areas are 280 and 320 K, respectively.

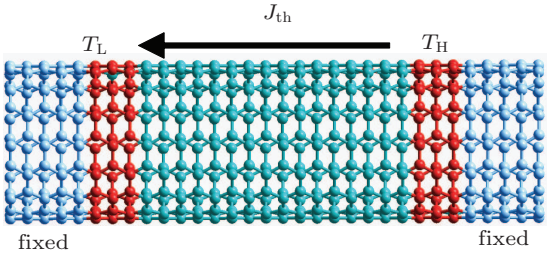


Fig. 4. (color online) Model of carbon nanotubes.

3. Simulation method

The thermal conductivity of carbon nanotubes with defects is numerically investigated by molecular dynamics (MD) simulation. The non-equilibrium molecular dynamics

(NEMD) method is employed, and the reactive empirical bond order (REBO) potential is chosen. In an REBO potential model, the total potential energy of the system is a sum of the nearest-neighbour pair interactions, which not only depend on the distance between atoms but also on their local atomic environment. A parameterized bond order function is used to describe chemical pair bonded interactions. Recently, the REBO model has been widely used in the studies concerning mechanical and thermal properties of carbon nanotubes.[17,18]

A total time of 1ns is employed for the simulation. An initial 0.5-ns simulation is performed for the equilibration with only temperature control. Then, calculation is carried out to obtain the temperature distribution (from 0.5 to 1 ns) and the energy budgets. The equations of motion in the simulation are solved by using the predictor–corrector algorithm, and the simulation is performed with a fixed time step $\Delta t = 0.5$ fs.

The temperature in the thermostat areas is given by using a Berendsen thermostat model,[19] and a thermostat coupling is accomplished by inserting stochastic and friction terms in the equations of motion.[20] While the temperature in the free part (the ambient temperature) is given by the Boltzmann energy equipartition theorem,[21] the temperature and heat flux along the tube are statistically average values and calculated as the simulation reaches a steady state.

The average temperature, which is calculated from the average kinetic energy of all atoms in the system, is expressed as follows:

$$T = \frac{\sum_{i=1}^{n} m_i v_i^2}{3Nk_{\mathrm{B}}}, \tag{1}$$

where n is the number of atoms, m_i is the atomic mass (in kg), v_i refers to the velocity of the i-th particle (in m/s), N is the Avogadro constant, and $k_{\mathrm{B}} = 1.38 \times 10^{-23}$ J/K is the Boltzmann constant.

The average heat flux q (in W/m^2) along the tube can be expressed as:

$$q = \frac{1}{A} \frac{\sum_{j=1}^{n} \Delta E(j)}{t_{\mathrm{s}}}, \tag{2}$$

where A is the cross-sectional area, t_{s} is the total time of simulation, and ΔE is the energy change in the thermostat area.

Then, the thermal conductivity of CNTs is obtained according to Fourier's law:

$$\lambda = -\frac{q}{\Delta T}, \tag{3}$$

where λ is the thermal conductivity (in W/m·K), and ΔT is the temperature gradient along the tube length.

4. Results and discussion

Forming mechanisms for SW and vacancy defects are similar. Both defects are caused by changing themselves in structures, leading to damage to the previously perfect hexagonal structure and reforming as a pentagon or heptagon structure. However, it is quite different from the doping defects produced by foreign atoms substituting for carbon atoms. We first discuss the doping defects individually, then we focus on both the SW and vacancy defects, which are compared with perfect tubes.

4.1. Doping defects

CNTs (10,10) of 12.7 nm in length with two-atom-doping defects are built. The thermal conductivities of doped CNTs are simulated under the ambient temperature rising from 200 to 600 K, as shown in Fig. 5.

Obviously, doping defects make the thermal conductivity of CNTs decrease, relative to the prefect tubes. From the theories of solid-state physics, new energy state density would be introduced around the CNT Fermi level due to doping defects. On one hand, it brings the CNT work function; on the other hand, it changes the electron emission densities which lead to different electron and phonon scatterings during the transport process, and finally results in lower thermal conductivities.

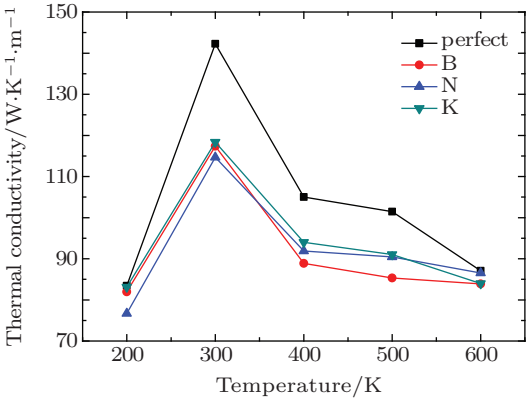


Fig. 5. (color online) Thermal conductivity of CNTs with different dopant types under different ambient temperatures.

The thermal conductivity presents an earlier rise and later decrease as the temperature rises in Fig. 5. Two factors function oppositely to the thermal conductivity of a phonon in a solid: 1) the solid heat capacity decreases when temperature declines, resulting in the drop of thermal conductivity; 2) the mean number of phonons goes down with decreasing temperature, and the mean free path of a phonon increases, so the thermal conductivity of the phonon rises. These two factors simultaneously restrict the one-way development of CNT thermal conductivity and create the peak values in a certain temperature range. The continuously rising temperature results in a higher shaking rate of the phonon and the decline of wavelength. The Umklapp scattering (U process) starts to occur and is strengthened with increasing temperature. This shortens the mean free path of the phonon and finally leads to a poorer performance in heat transfer. This is the reason why

thermal conductivity goes down when the temperature grows at a relatively high temperature.

The thermal conductivity of single-walled carbon nanotubes changes with different defect concentration. Figure 6 presents the rising of concentration from 0 (i.e., a perfect tube without defects) to 0.46%, while the thermal conductivities keep falling. The results show that thermal conductivities decrease by about 37%, 33%, and 36%, corresponding to B-, N-, and K-doping defects, respectively.

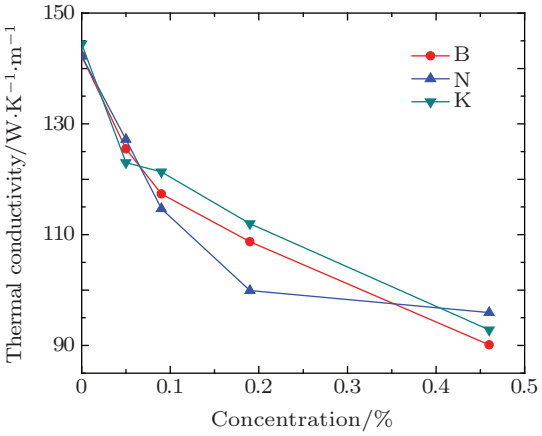


Fig. 6. (color online) Thermal conductivity of CNTs with different dopant defect concentrations.

From Figs. 5 and 6, we can see that the thermal conductivity of CNTs doped with B, N, and K shows a similar tendency, so further analysis of doping effects is focused on some typical B-doped CNTs.

The effects of the tube length are considered under the same doping concentration of 0.09% of B atoms. The thermal conductivities of CNTs (10, 10) with tube lengths from 65.2 to 347.7 Å are simulated. The results are compared with perfect ones in Fig. 7.

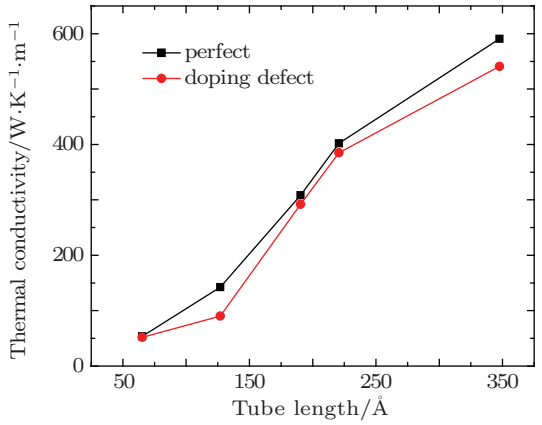


Fig. 7. (color online) Thermal conductivity of B-doped CNTs with different lengths.

The result shows an obvious size effect and a ballistic effect of thermal conductivity for CNTs due to its quite long phonon mean free path. This is not only because the perfect quasi-one-dimensional structure of CNTs can limit phonon scattering, but also because the sp^2 C–C covalent bonding can lead to a higher speed of sound. The thermal conductivity of doped CNTs has grown along with the tube length, showing a good agreement with the perfect CNTs under the size effects, and seems not to be related to doping.

The size effects of thermal conductivity for CNTs were also studied by the authors in Refs. [22] and [23] based on Boltzmann equation and Landau transport theory, respectively. They both concluded that the thermal conductivity of CNTs increase with the length growing. The authors in Refs. [24] and [25] found that the thermal conductivity of CNTs would be distributed exponentially (index is commonly 2/5 or 1/3) with the tube length. Some other researchers believe that the heat conduction could fully realize diffusion and transportation, thus the thermal conductivity would finally converge at a fixed value with growing tube length. By solving the ballistic transport function, Mingo also drew the conclusion that the CNTs possess a long ballistic length.[26] In order to gain the convergent thermal conductivity in our MD simulation, longer CNTs should be focused upon.

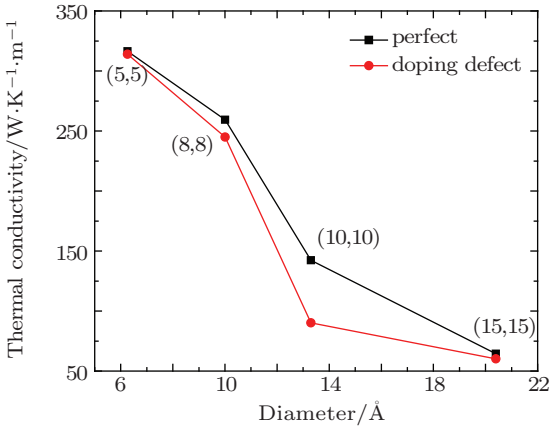


Fig. 8. (color online) Thermal conductivity of B-doped CNTs of different diameters.

The effectiveness of different tube diameters is also investigated. The diameter changing is reflected by the following different armchair nanotubes: (5,5), (8,8), (10,10), and (15,15). The B-doped CNTs with thermal conductivities of 0.09% are shown in Fig. 8. It implies that the thermal conductivity decreases as the diameter increases in both doped CNTs and perfect CNTs. This finding agrees with the theoretical results from the Ballistic transport equation by Mingo.[22] For larger diameters, strenuous exercise of atoms is much easier to be set free. Accordingly, the thermal conductivity declines. The lattice dynamics study by Yan *et al.*,[27] suggests that the smaller the diameter is, the lower the chance of three-phonon U scattering is, and the better the performance of heat transfer is. The vibrational mode in CNTs is related to its structural index. For instance, the phonon branches of total vibrational mode for (5,5) CNTs is 60, while reaches 120 in (10,10)

CNTs. Hence, the three-phonon U scattering in (10,10) tubes is stronger than in (5,5) tubes, so its thermal conductivity is lower than that of (5,5) tubes. It is accordingly estimated that the thermal conductivity of 4 Å in diameter would reach an ultrahigh value, owing to the significant geometry restrictions on the U process. Different chiralities also have an impact on the thermal conductivity of CNTs when doping happens. B-doped CNTs with thermal conductivities of 0.09% are compared with perfect ones under three different kinds of chiralities, including armchair (10,10), zigzag (10,0), and helicity (5,3). The results are shown in Fig. 9. Apparently, the most appreciable changes take place in the armchair CNTs by a 44% decline in thermal conductivity with doping defects. However, doping defects have much less influence on zigzag CNTs.

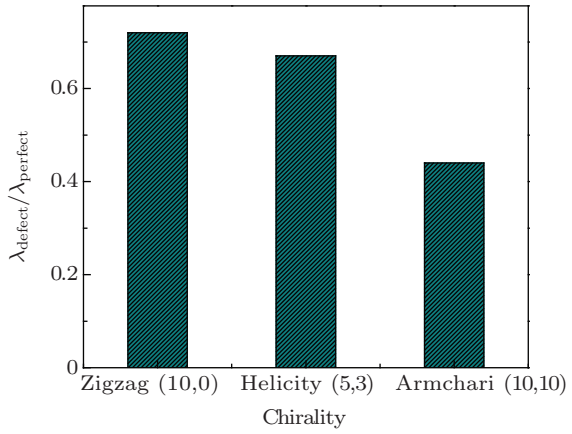


Fig. 9. (color online) Thermal conductivity of B-doped CNTs with different chiralities.

4.2. SW and vacancy defects

The thermal conductivity of (10,10) CNTs of 12.7 nm in length with an SW or a vacancy defect concentration of 0.14% is illustrated in Fig. 10, under different ambient temperatures. Compared with a perfect tube possessing an unusually high thermal conductivity due to its wonderful one-dimensional nanostructure without atomic defects, either an SW or a vacancy defect will make the thermal conductivity decrease, while there is a more dramatic drop for the SW situation.

The thermal conductivity increases first and then decreases with increasing temperature. This behavior produces a peak value at a temperature between 300 and 400 K. The appearance of peak is due to the same reason as stated in the doping situation. However, the peak for SW or vacancy CNTs is not as apparent as in perfect tubes, especially under vacancy defects. The quantization of the phonons along the circumference is possibly responsible for these different thermal conductivity behaviors. When SW or vacancy defects are introduced, the structure along the circumference of the nanotube is destroyed, causing partial reconfiguration, which has an impact on the quantization of the phonons along the circumference. It leads to a change of the phonon dispersion. Finally, the thermal conductivity shows a different reaction to temperature, compared with perfect CNTs. However, results from CNTs with doping defects are much more similar to the perfect tubes, with a sharp peak at the same temperature (see Fig. 5). The possible reason for this may be: doping is realized by replacing the positions of carbon atoms with some foreign atoms, and the original hexagons are retained. However, SW or vacancy defects can totally break the structure of carbon hexagons and then the carbon atoms can connect to form other shapes which form a completely different structure.

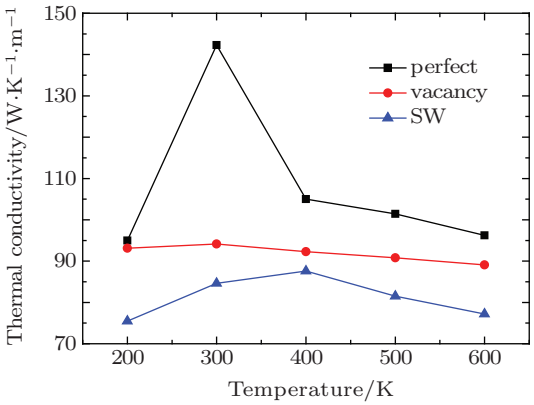


Fig. 10. (color online) Thermal conductivity of CNTs with vacancy/SW defects under different temperatures.

Figure 11 illustrates the thermal conductivity of CNTs with different defect concentration at an ambient temperature of 300 K. When one defect is introduced into the tube, the thermal conductivity shows a sharp decline, and the thermal conductivity continues to decrease with the defect concentration increasing. The defects break the perfect structure, and more defects (larger defect concentration) cause more reduction in the nanotube's thermal conductivity.

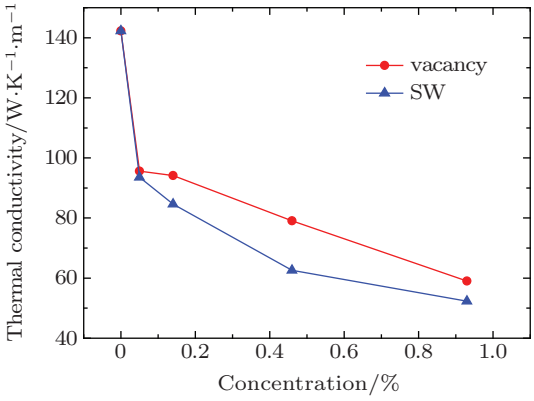


Fig. 11. (color online) Thermal conductivity of CNTs with SW/vacancy defects under different defect concentrations.

Figure 12 presents the thermal conductivity of (10,10) CNTs varying with tube length. Either in perfect tubes or tubes with certain defects, the thermal conductivity increases with the tube length, but CNTs with SW defects begin to converge after 127 Å. It is interesting that the length of thermal

conductivity convergence for CNTs with SW defects seems to be much shorter than for perfect and vacancy tubes.

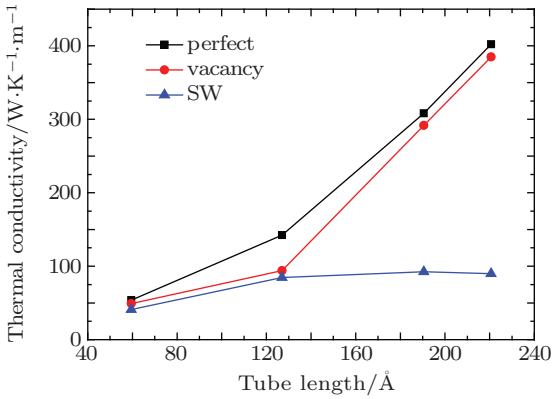


Fig. 12. (color online) Thermal conductivity of CNTs with SW/vacancy defects under different lengths.

While magnifying the tube diameter, the thermal conductivity of CNTs with different chiralities, including (5,5), (8,8), (10,10), (15,15), and (20,20), is calculated, respectively. Results are presented in Fig. 13, which exhibits that thermal conductivity of CNTs goes down when the diameter increases. The SW or vacancy tubes are less sensitive to the diameter change than perfect ones.

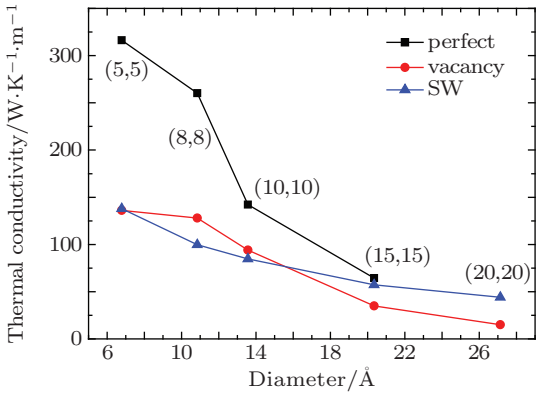


Fig. 13. (color online) Thermal conductivity of CNTs of different diameters with SW/vacancy defects.

Zigzag nanotube (10,0) and armchair nanotube (10,10) are used to observe the sensitivities of defects to chirality. The defect concentration is 0.14%. Results are shown in Fig. 14. From this bar chart, we can find that the thermal conductivity of CNTs with vacancy defects drops much more obviously in zigzag tubes than in armchair ones. Furthermore, vacancies have a more obvious influence than the SW defect in zigzag tubes. However, in armchair tubes, the condition is reversed. According to Fig. 9, doping defects are most influential within armchair nanotubes. These results imply that the type of defects would lead to the thermal conductivity of CNTs under different chiralities to vary widely.

In line with present theoretical studies, we would like to point out that more abnormal phenomena could possibly be predicted in the thermal transport of carbon nanotubes, if the defect effect is further analyzed with surface effect, quantum scale effect, and macro-quantum tunnel effect. We still have much work to do.

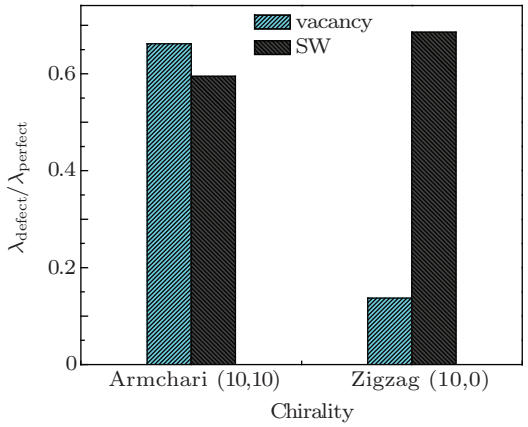


Fig. 14. (color online) Thermal conductivity of CNTs with SW/vacancy defects under different chiralities.

5. Conclusions

The non-equilibrium molecular dynamics method is applied to simulate the thermal conductivity of CNTs with doping, SW, and vacancy defects. Results are compared with perfect CNTs for analyzing the influence mechanisms of factors such as tube length, diameter, chirality, and the ambient temperature, coupled with defects contributions. We list the conclusions as follows.

(i) Defects in CNTs lead to a poor thermal conductivity performance.

(ii) With the temperature rising, thermal conductivity of defective CNTs presents a trend of ascending to a peak, and then declining. The temperature at which the peak occurs varies with the defect type. The peak for SW or vacancy tubes is not as apparent as perfect and doped ones, especially under vacancy defects.

(iii) The thermal conductivity grows with increasing tube length or decreasing diameter. The length of thermal conductivity convergence for a SW tube is much shorter than a perfect or a vacancy tube. The SW or vacancy tubes are less sensitive to the diameter change than perfect ones.

(iv) Doping and SW defects have greater effects on armchair tubes, while vacancy defects affect zigzag tubes more.

References

[1] Iijima S 1991 *Nature* **354** 56
[2] Deng F, Zheng Q S, Wang L F and Nan C W 2007 *Appl. Phys. Lett.* **90** 021914
[3] Ujereh S, Fisher T and Mudawar I 2007 *Int. J. Heat Mass Transfer* **50** 4023
[4] Meunier V and Lambin P H 2000 *Carbon* **38** 1729
[5] Nardelli B M, Fattebert J L, Orlikowski D, Roland C, Zhao Q and Bernholc J 2000 *Carbon* **38** 1703

[6] Cummings A, Osman M, Srivastava D and Menon M 2004 *Phys. Rev.* B **70** 115405
[7] Meng F Y, Ogata S, Xu D S, Shibutani Y and Shi S Q 2007 *Phys. Rev.* B **75** 205403
[8] Bi K, Chen Y and Yang J 2006 *Phys. Lett.* A **350** 150
[9] Che J, Cağin T and Goddard III W 2000 *Nanotechnology* **11** 65
[10] Kondo N, Yamamoto T and Watanabe K 2006 *e-J. Surf. Sci. Nanotech.* **4** 239
[11] Zhang G and Li B 2005 *J. Chem. Phys.* **123** 114714
[12] Li W, Feng Y H, Zhang X X and Chen Y 2012 *Acta Phys. Sin.* **61** (in Chinese)
[13] Jin L, Fu H G, Xie Y and Yu H T 2012 *Chin. Phys.* B **21** 057901
[14] Wang Y J, Wang L D, Yang M and Yan C 2011 *Chin. Phys.* B **20** 117304
[15] Zhang L J, Hu H F, Wang Z Y, Chen N T, Xie N and Lin B 2011 *Acta Phys. Sin.* **60** 077209 (in Chinese)
[16] Luo Y P, Tien L G, Tsai C H, Lee M H and Li F Y 2011 *Chin. Phys.* B **20** 087303
[17] Brenner D W, Shenderova O A, Harrison J A, Stuart S J, Ni B and Sinnott S B 2002 *J. Phys.: Condens. Matter* **14** 783
[18] Bao W X, Zhu C C and Cui W Z 2004 *Physica* B **352** 156
[19] Berendsen H J C, Postma J P M, Gunsteren W F, Dinola A and Haak J R 1984 *J. Chem. Phys.* **81** 3684
[20] Schneider T and Stoll E 1978 *Phys. Rev.* B **17** 1302
[21] Allen M P and Tildesley D J 1987 *Computer Simulation of Liquids* (Oxford: Clarendon Press)
[22] Mingo N 2005 *Nano Lett.* **5** 1221
[23] Wang J and Wang J S 2006 *Appl. Phys. Lett.* **88** 111909
[24] Shiomi J and Maruyama S 2008 *Phys. Rev.* B **78** 205406
[25] Maruyama S, Kojima R, Miyauchi Y, Chiashi S and Kohno M 2002 *Chem. Phys. Lett.* **360** 229
[26] Mingo N 2005 *Phys. Rev. Lett.* **95** 096105
[27] Yan X H, Xiao Y and Li Z M 2006 *J. Appl. Phys.* **99** 124305